15

Improving Elastic Properties of Polymer-Reinforced Aerogels

Mary Ann B. Meador

Abstract Monolithic aerogels provide superior thermal insulation compared to other forms of aerogel (composites, particulate, etc.). It has also been demonstrated that monolithic aerogels can be made mechanically stronger and more durable by incorporating a conformal polymer coating on the skeletal nanostructure. However, for many applications it would be most desirable to have monolithic aerogels in a more flexible form, for example, as insulation in deployable and inflatable structures or space suits, or to wrap around a structure needing insulation. To this end, it has been found that by incorporating organic linking groups or alkyl trialkoxysilanes into the silica backbone, elastic recovery and/or flexibility is improved, while strength is maintained by the use of polymer reinforcement.

15.1. Introduction

Due to their combination of low density, high porosity, high surface area, and nanoscale pore sizes, silica aerogels are of interest for many applications including thermal and acoustic insulation, optics, catalysis, and chromatographic systems [1–3] (Chap. 2). However, potential applications of aerogel monoliths in aerospace, industry, and daily life have been restricted due to their poor mechanical properties and their extreme fragility [4]. Hence, in aerospace, especially (Chaps. 32 and 33), aerogel monoliths have been limited to a few exotic applications such as collecting hypervelocity particles from the tail of the comet Wild 2 in the Stardust Program [5] and as thermal insulation on the Mars Rover [6].

It has been shown that reinforcing silica aerogels by reacting polymer with the silanol surface to create a conformal coating over the silica skeleton is an effective way to increase mechanical strength by as much as two orders of magnitude while only doubling the density over those of native or nonreinforced aerogels [7–9] (Chap. 13). In addition, the mesoporosity of these polymer-reinforced aerogels, and hence, their superior insulation properties among other things, is maintained. Incorporating an amine onto the surface of the silica gel particles by coreacting the tetraalkoxysilane with 3-aminopropyltriethoxysilane (*APTES*), as shown in Scheme 15.1, allows for reinforcement with epoxy-terminated oligomers [10, 11] or cyanoacrylates [12] and also improves the reactivity of the silica surface toward

M. A. B. Meador • NASA Glenn Research Center, Mailstop 49-3, Cleveland, OH 44135, USA
e-mail: maryann.meador@nasa.gov

M.A. Aegerter et al. (eds.), *Aerogels Handbook*, Advances in Sol-Gel Derived Materials and Technologies, DOI 10.1007/978-1-4419-7589-8_15,

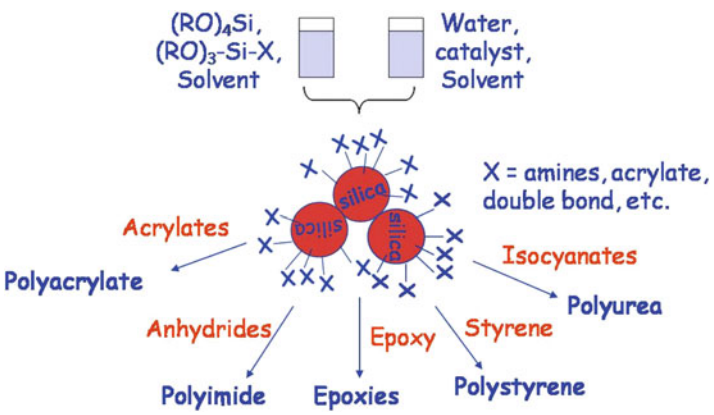

Scheme 15.1. Concept of polymer reinforcement using reactive groups on the silica surface.

isocyanates [13–15]. Expanding the silica surface chemistry to include styrene groups [16], free radical initiator [17] or vinyl [18] permits the use of polystyrene as a cross-linker. Other approaches to strengthening the silica aerogel structure by incorporation of a polymer include dispersing functionalized polymer nanoparticles in a silica network [19] (Chap. 21) and copolymerization of silica precursors with poly(methylmethacrylate) or poly(dimethylacryl-amide) [20] or poly(vinylpyrrolidone) [21].

Improvements to mechanical properties (Chap. 22) seen by reinforcing aerogels with polymer enable a whole host of weight-sensitive aerospace applications, including thermal and acoustic insulation for habitats, extravehicular activity (*EVA*) suits, launch vehicles, cryotanks, and inflatable decelerators for planetary reentry, as well as lightweight, multi-functional structures (including insulation, sound dampening, and structural support) for aircraft or rotorcraft. In addition, if manufacturing costs of polymer-cross-linked monolithic aerogel can be decreased, down to earth applications, including insulation for refrigeration, housing construction, and industrial pipelines, can be realized.

In particular, manned Mars surface applications shown in Figure 15.1 absolutely require a new insulation system. Multilayer insulation (*MLI*), usually consisting of many thin layers of polymer such as Kapton or Mylar metalized on one side with aluminum or silver, requires a high vacuum to be effective. In evacuated conditions, contact points between the separate layers in *MLI* are reduced. Hence, conduction and convection are minimized. The multiple layers reduce the last form of heat transfer, radiation, by radiating and absorbing heat from each other, effectively trapping most of the thermal energy (Chap. 23). The high vacuum required for *MLI* to be an effective insulation is abundantly available in the lunar environment and earth orbit. Mars, on the other hand, has an atmosphere consisting of mostly CO_2 with an average surface pressure of 6 torr [22]. The target thermal conductivity of materials for Mars *EVA* suits is 5 mW/m-K. Of a variety of composite materials considered in a recent study, only aerogel fiber composites come close to meeting that goal [23]. A monolithic polymer-reinforced aerogel may meet this goal, but insulation for *EVA* suits should also be durable and flexible to accommodate as much freedom of movement for the astronaut as possible. Flexible fiber-reinforced silica aerogel composite blankets were recently evaluated using thermal and mechanical cycling tests for possible use in advanced *EVA* suits [24]. During testing, thermal conductivity did not change much, but the composite aerogels were found to shed silica dust particles at unacceptable levels. Polymer reinforcement may also be a means to reduce shedding.

Figure 15.1. NASA vision of manned mission to Mars surface activities. (Reprinted with permission from SAE paper 2006-01-2235 © 2006 SAE International.)

A flexible form of polymer-reinforced aerogel would also be desirable for wrapping around structures that need to be insulated, such as cryotanks or cryogenic transfer lines. Currently, expendable cryotanks, such as the Space Shuttle's external liquid oxygen/hydrogen tank, use spray-on polyurethane foam to insulate the tank on the launch pad. Cryogenic tanks employed in space generally utilize the same *MLI* as space suits, but require additional insulation while on the launch pad since the *MLI* is not an effective insulator under ambient pressure as discussed previously. An aerogel insulation system can function reliably in both ambient pressure and high vacuum, making foam insulation unnecessary [25]. However, molding a net shape aerogel to fit around a structure can be difficult since complex molds need to be devised and the gels before polymer cross-linking can be quite fragile.

Another use for flexible durable aerogels could be as part of an inflatable decelerator used to slow spacecraft for planetary entry, descent, and landing (*EDL*) as shown in Figure 15.2 [26]. *EDL* systems used to successfully land six robotic missions on Mars from 1976 to 2008 employed a hard aeroshell heat shield and parachutes of 12–16 m in diameter. Future robotic and manned missions are much heavier and will require more drag for landing. Hence, new designs with much larger diameters (30–60 m) will be required [27]. Inflatable decelerators would stow in a small space and deploy into a large area lightweight heat shield to survive reentry [28]. Minimizing weight and thickness of the system as well as providing suitable insulation are important considerations.

Polymer-reinforced aerogels are somewhat flexible at densities below 0.05 g/cm^3, but mechanical strength is reduced at these densities [14]. However, much more flexibility can be obtained in aerogels by altering the silica backbone in some significant way. For example, Kramer et al. [29] demonstrated that including up to 20 w/w% polydimethylsiloxane (*PDMS*) in tetraethyl orthosilicate (*TEOS*)-based aerogels resulted in rubbery behavior with up to 30% recoverable compressive strain. More recently, Rao et al. [30] have demonstrated that utilizing methyltrimethoxysilane (*MTMS*) as the silica precursor and a two-step synthesis imparts extraordinary flexibility to the aerogels. The *MTMS*-derived aerogels are more flexible largely because of the resulting lower cross-link density of the silica (three alkoxy groups that can react vs. four in rigid *TMOS*- or *TEOS*-derived aerogels).

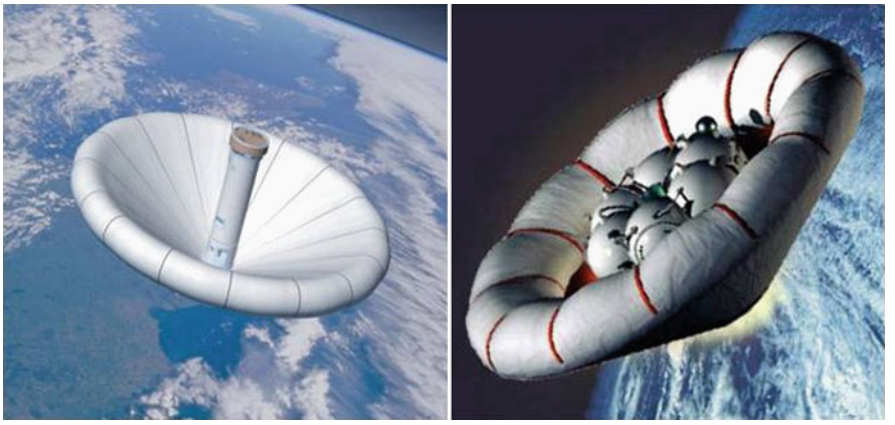

Figure 15.2. Inflatable decelerator concepts. Courtesy of the Inflatable Re-entry Vehicle Experiment (IRVE) Project.

Kanamori et al. [31], using a surfactant to control pore size and a slightly different process, have shown that *MTMS*-derived gels demonstrate reversible deformation on compression. In fact, some formulations were able to be dried ambiently. Initially, the gels shrink about 65% but spring back to nearly their original size, resulting in nearly the same density and pore structure as those dried supercritically.

Though the *MTMS*-derived aerogels are very flexible and elastic, it does not take much force to compress them. For example, Rao [28] reports a Young's modulus of only 0.03–0.06 MPa for the flexible *MTMS*-derived aerogels ranging in density from 0.04 to 0.1 g/cm^3. Kanamori [29] does not report Young's modulus, but stress–strain curves indicate that stresses of less than 1 MPa are sufficient to compress samples with bulk densities around 0.2 g/cm^3 to 25% strain.

Shea and Loy have employed bridged bis(trialkoxysilyl) monomers as precursors for silsesquioxane-derived aerogels and xerogels [32, 33]. Typically, this allowed for control of pore size directly related to the size of the bridge, with the best results obtained using a stiffer structure such as an arylene chain. More flexible bridges such as alkyl chains resulted in more compliant aerogels but tended to shrink more, reducing porosity.

More recently, we have been combining the notion of altering the underlying silica structure to add flexibility and elastic behavior and the notion of polymer reinforcement to add strength and durability. This is accomplished by substituting some of the *TEOS* or *TMOS* with organic bridged bis(trialkoxysilanes) or with *MTMS*. This work, which has been shown to be a versatile method of imparting more elastic behavior and flexibility to the aerogels, is summarized herein.

15.2. Hexyl-Linked Polymer-Reinforced Silica Aerogels

15.2.1. Di-isocyanate-Reinforced Aerogels

Silica aerogels reinforced with di-isocyanate through aminopropyl groups on the silica surface are made as shown in Scheme 15.2, where APTES and *TMOS* or *TEOS* are coreacted in acetonitrile to form a wet gel [13]. After being washed several times to remove water and alcoholic by-products of gelation, the wet gel is subsequently soaked in a solution of

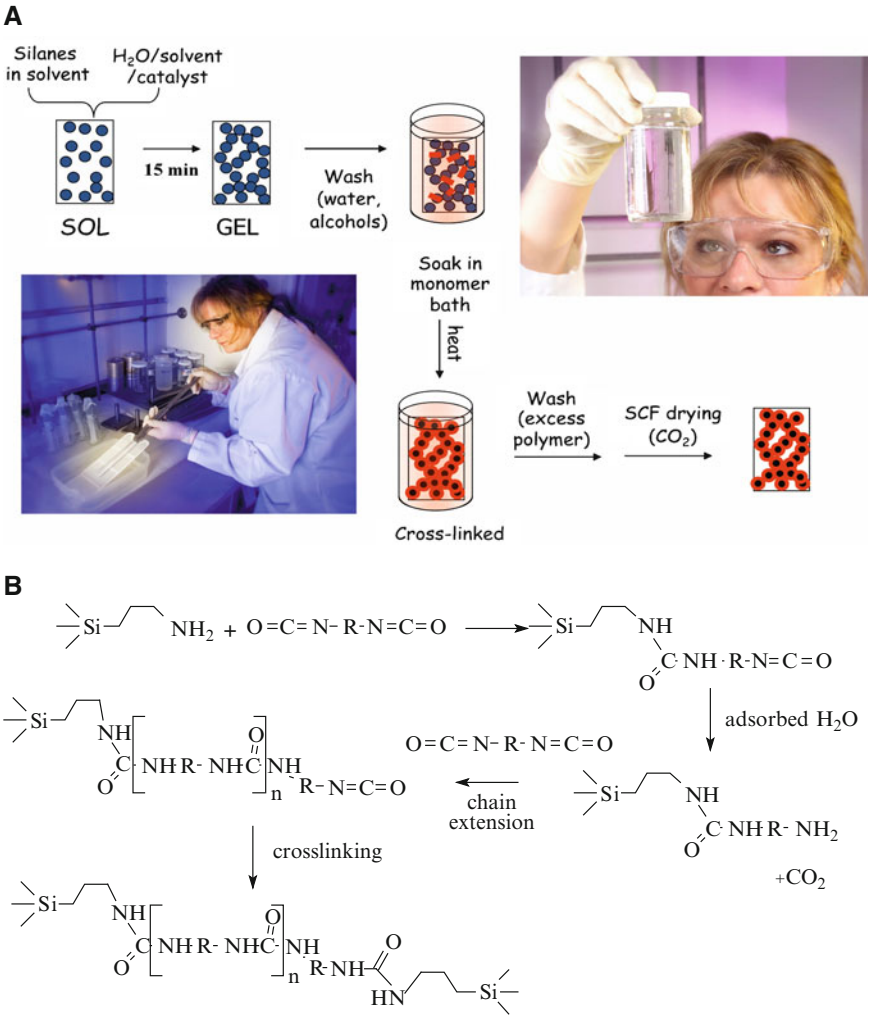

Scheme 15.2. Fabrication of polymer-reinforced aerogels **A.** and mechanism of di-isocyanate crosslinking **B.**

Desmodur N3200 [34], an oligomeric form of hexamethylene di-isocyanate (*HDI*). Heating causes reaction of the isocyanates with surface amines as shown in Scheme 15.2B. The length of the polyurea cross-links depends on both the di-isocyanate concentration in the soak solution and the amount of residual water from the hydrolysis left in the gels. This is because isocyanate reacts with water to generate an amine that can react with other isocyanates to cause chain extension.

Hexyl linkages can be incorporated into the wet gels by replacing some of the *TMOS* or *TEOS* with 1,6-bis(trimethoxysilyl)hexane (*BTMSH*), noting that each *BTMSH* molecule contributes two atoms of Si [35]. Scheme 15.3 shows a comparison of the silica gel structure (a) with 20 mol% APTES-derived Si and no hexyl linkages incorporated and (b) with about 40 mol% Si derived from *BTMSH*. A comparison of the silica gel structure with and without hexyl links is shown in Scheme 15.3. Note that the hexyl linkages serve to open up the structure and effectively reduce in size the regions of rigid silica.

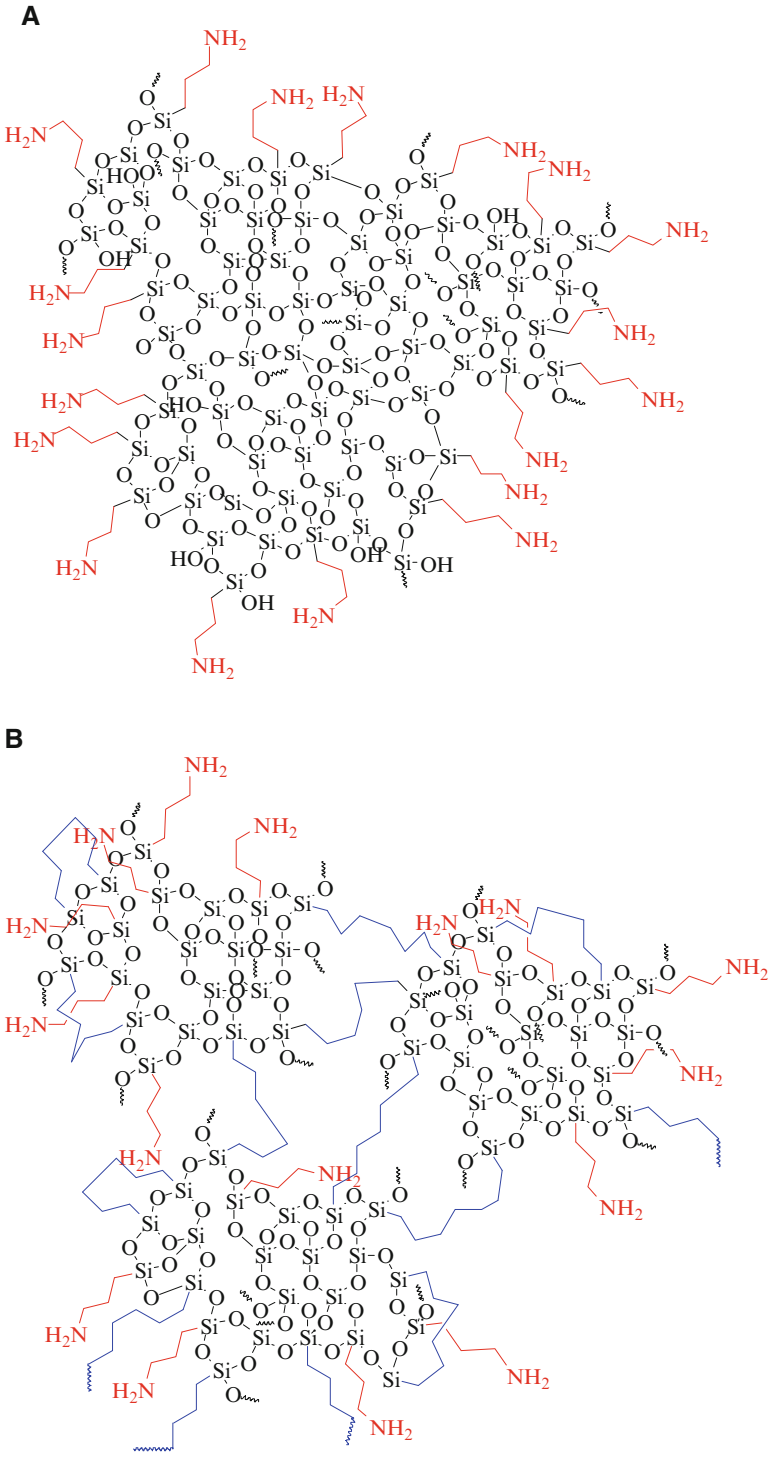

Scheme 15.3. Underlying silica backbone structure made using **A.** 20 mol% APTES and **B.** 20 mol% APTES with 40 mol% BTMSH-derived Si. Reprinted from [11], Copyright 2009 American Chemical Society.

Wet gels prepared with *BTMSH* are more resilient and easier to handle than those containing no *BTMSH* even at low silane concentrations, bending as they come out of a mold instead of breaking. Hence, the use of *BTMSH* can possibly improve the manufacturability of the aerogels. After reaction with di-isocyanate, the wet gel is resilient enough to be bent and manipulated to a great extent without breaking as shown in Figure 15.3. The resulting aerogels after drying with supercritical CO_2 can also be bent without breaking, but not to the same extent as the wet gels. This is due to a reduced plasticization of the silica/polymer network by the removal of the solvent.

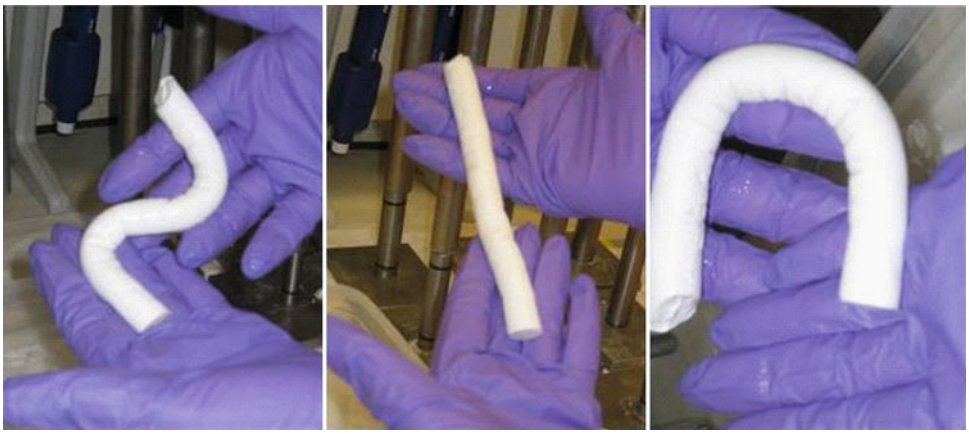

Figure 15.3. A di-isocyanate-reinforced wet gel with 35 mol% BTMSH-derived Si and 30 mol% Si from APTES is shown to be flexible and resilient before drying.

Inclusion of hexyl links does have an effect on the pore structure. As shown in Figure 15.4, the average pore diameter as measured by nitrogen sorption using the Brannauer–Emmet–Teller (BET) method is around 18 nm with a sharp pore size distribution for higher density di-isocyanate-reinforced aerogels containing no *BTMSH*. The average pore size increases and the pore size distribution broadens as silicon concentration is decreased.

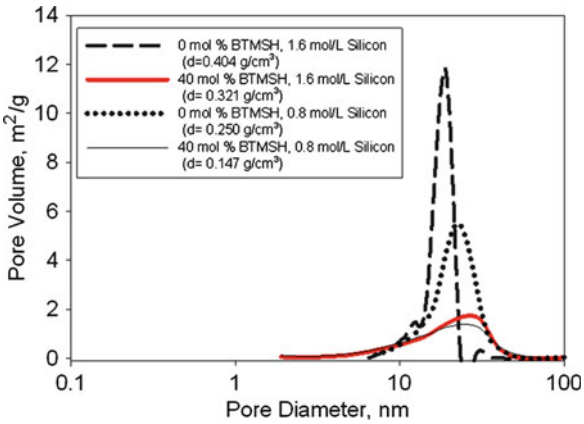

Figure 15.4. Pore volume vs. pore diameter plot for di-isocyanate-reinforced aerogels made using varying amounts of total silane concentration and mol% BTMSH-derived Si.

15.2.2. Styrene-Reinforced Aerogels

Several approaches to reinforcing silica aerogel with styrene have been studied, including incorporation of styrene [16], a free radical initiator [17], or a vinyl [18] on the silica surface. All of these approaches result in greater hydrophobicity (Chap. 3), and improvements in mechanical strength over non-cross-linked silica aerogels. A series of vinyl decorated silica gels have been fabricated by coreacting vinyltrimethoxysilane (*VTMS*), *BTMSH*, and *TMOS* in alcohol solution. Up to 50% of the *TMOS*-derived Si atoms are replaced with *BTMSH*-derived Si, noting again that each *BTMSH* contributes two atoms of Si. As shown in Scheme 15.4A, the proposed silica gel structure is similar to that previously shown for the APTES-derived structure except with a vinyl decorated surface.

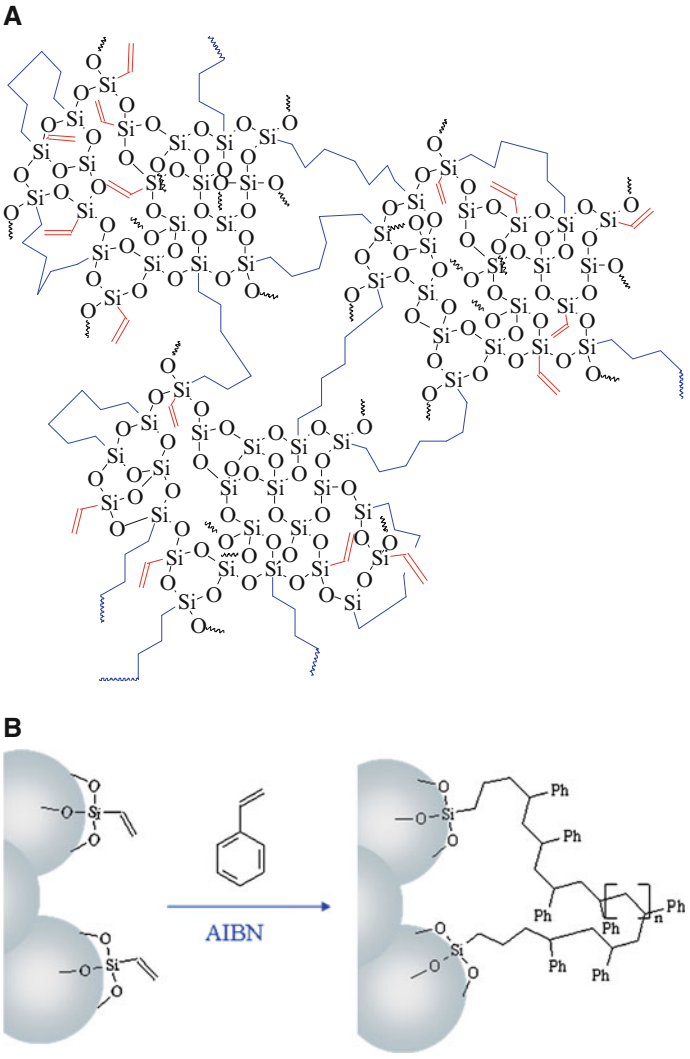

Scheme 15.4. Silica structure incorporating hexyl links and vinyl groups for reinforcement with polystyrene. Reprinted from [18], Copyright 2009 American Chemical Society.

Cross-linking with styrene is carried out as shown in Scheme 15.4B after exchanging solvent from methanol or ethanol to chlorobenzene and soaking the wet gels in a solution of styrene monomer and radical initiator.

As a way of characterizing elastic properties (Chap. 22), styrene-reinforced aerogel monoliths are taken through two successive compression cycles to 25% strain. Stress–strain curves of successive compression tests of polymer-reinforced aerogels without hexyl-linking groups in the underlying silica typically look like that shown in Figure 15.5A. The first compression is taken to 25% strain and released and followed immediately by a second compression to 25% strain. Between the first and second compression, about 13% of the length of the sample is not recovered. In contrast, Figure 15.5B shows repeat compression tests of a styrene-reinforced aerogel made with 49 mol% of Si derived from *BTMSH*, 29 mol % derived from *VTMS*, and 22 mol% from *TMOS*. In this case, the first and second compression curves almost overlap. Nearly, all the length (99.5%) is recovered within 30 min after the second compression as shown in Figure 15.5C. Note that the compressive modulus of this hexyl-linked aerogel is over 3 MPa.

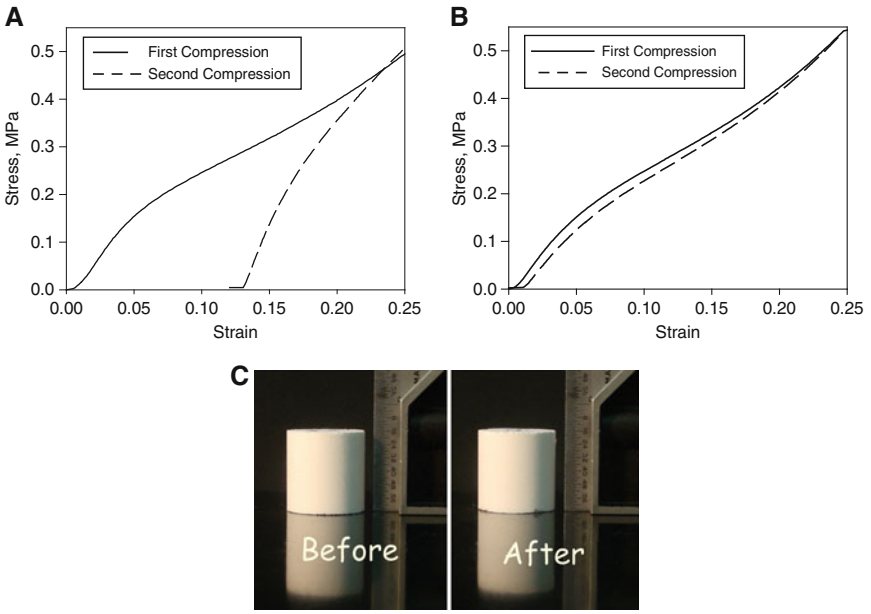

Figure 15.5. Repeat compression cycles of **A.** a styrene-reinforced aerogel monolith without flexible linking groups and (density = 0.122g/cm^3, surface area = 366 m^2/g); **B**. a styrene-reinforced monolith with 49 mol% Si derived from hexyl-linked BTMSH (density = 0.232 g/cm^3, surface area = 158 m^2/g; and **C.** the monolith from **B.** before and after two compressions. Reprinted from [18], Copyright 2009 American Chemical Society.

Interestingly, hexyl-linking groups also improve the hydrophobicity of the polystyrene-reinforced aerogels. Water droplet contact angles of styrene-reinforced aerogels have been reported to be in the range of 112–120° for samples containing no *BTMSH*. Samples with at least 29 mol% *BTMSH*-derived Si had water droplet contact angles ranging from 127 to 138°. This indicates that the hexyl group from *BTMSH* is also present on the silica surface and has a significant effect on the hydrophobic nature of the aerogels above and beyond the simple polystyrene cross-linking.

15.2.3. Epoxy-Reinforced Aerogels from Ethanol Solvent

Previously, the type of polymer reinforcement has dictated the solvent choice based on the solubility of the monomers and cure temperature of the cross-linking chemistry. In order to scale up manufacturing processes for cross-linking aerogels, it is desirable to adopt a more industrially friendly solvent. It has been demonstrated that less toxic *TEOS* and ethanol can be used to synthesize polymer-reinforced silica aerogels by cross-linking ethanol-soluble epoxies with APTES-derived amine groups (Scheme 15.5). In this manner, similar increases in mechanical properties were achieved in comparison to previously studied isocyanate cross-linked aerogels [11]. The use of ethanol as solvent in particular improves the viability of large-scale manufacturing of the polymer-cross-linked aerogels since large amounts of solvent (from initial gelation through diffusion of monomer into the alcogels and additional rinsing steps) are used in the production.

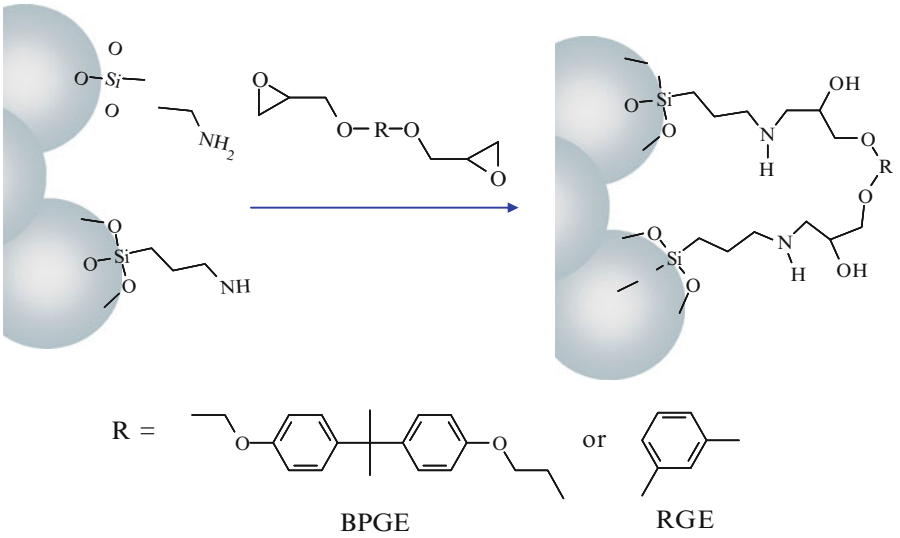

Scheme 15.5. Typical reaction scheme for crosslinking silica gels with epoxy through surface amine groups (reprinted from [11], Copyright 2009 American Chemical Society).

Varying total silane concentration and the mole fraction of APTES and *BTMSH* leads to aerogels with different pore structures as seen with both the styrene- and di-isocyanate-reinforced aerogels. Figure 15.6 shows scanning electron micrographs of four aerogel monoliths made using 15 mol% APTES. The top samples (Figure 15.6A, B) are made using 1.6 mol/l total silicon. The sample shown on the left (Figure 15.6A) is made using no *BTMSH*, while the right-hand sample (Figure 15.6B) is made using 40 mol% of Si derived from *BTMSH*. Both samples show a fine distribution of similar size particles, but in the sample containing hexyl links (Figure 15.6B), pores appear to be larger. The density of the hexyl-linked samples is also smaller, though the two samples are made with the same total moles of silicon, the same amount of amine, and the same concentration of epoxy.

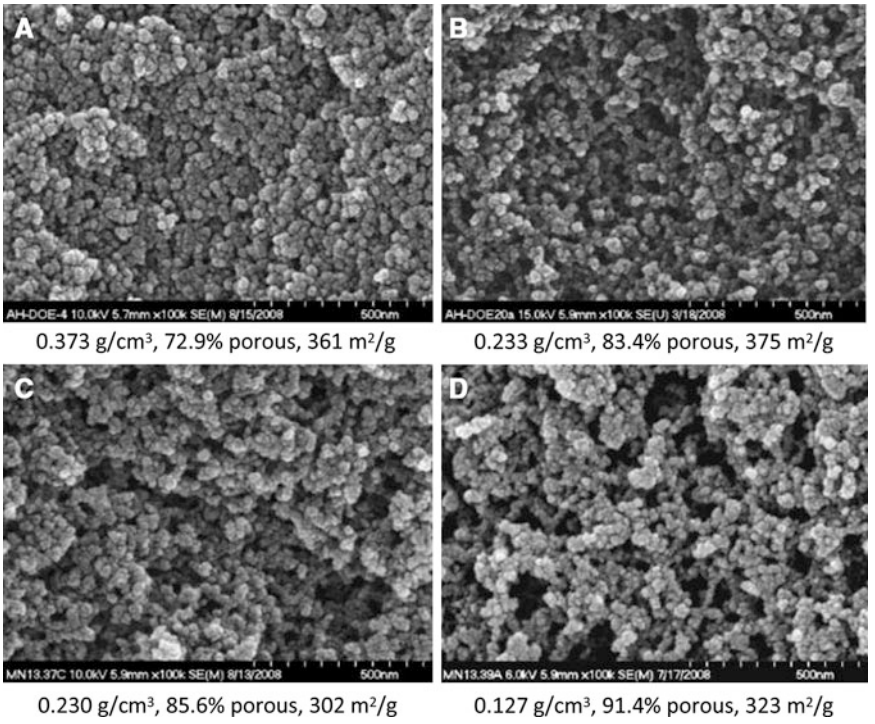

Figure 15.6. Side-by-side comparisons of micrographs of samples with (*left*) no BTMSH and (*right*) 40 mol% BTMSH-derived Si, including samples prepared with 1.6 mol/l total Si (15 mol% APTES) **A.** and **B.**; and with 0.8 mol/l total Si (15 mol% APTES) (**C** and **D**). Reprinted from [11], Copyright 2009 American Chemical Society.

The density difference is due to the fact that hexyl-linked samples tend to shrink less during processing. A similar but more pronounced effect is seen for samples made using 0.8 mol/l total silicon (Figure 15.6C, D). Again, the particle sizes are similar between the two samples, but larger pores are evident in the hexyl-linked sample shown in Figure 15.6D and the density is lower. However, BET surface areas are fairly constant for all four samples – only the distribution of pore sizes changes with *BTMSH* concentration.

Empirical models were generated for predicting properties of the epoxy-cross-linked aerogels over a wide range of densities as well as to identify and understand significant relationships between the processing parameters and final properties. Figure 15.7 exhibits empirical models for (a) density, (b) Young's modulus from compression tests, and (c) amount of recovery after compression to 25% strain. As seen in Figure 15.7A, highest density is seen when using 1.6 mol/l total Si and APTES-derived Si is 45 mol%. At the same time, Figure 15.7B shows that highest modulus (95 MPa), when no *BTMSH* is used, is achieved with APTES-derived Si at about 30 mol%.

Using *BTMSH* does appear to lower modulus with optimum modulus in this system (~40 MPa) being produced in combination with 45 mol% APTES. However, this change in modulus is at least in part due to the decrease in shrinkage (and concomitant decrease in density) using higher *BTMSH* concentrations.

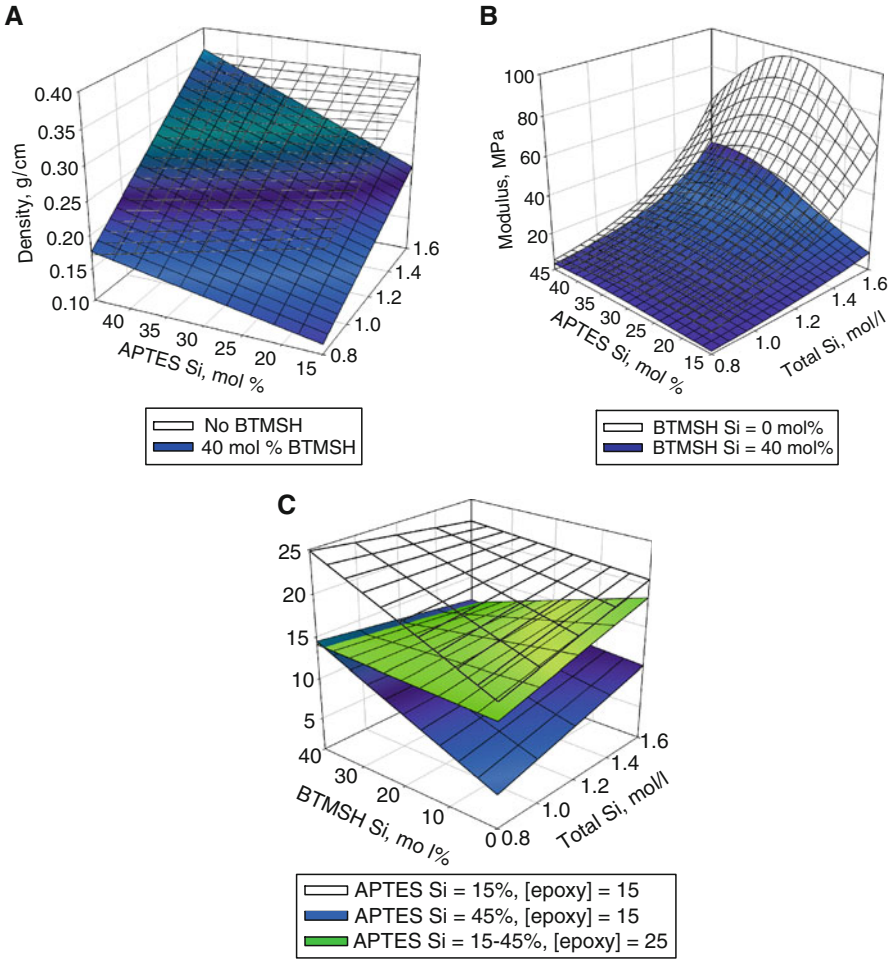

Figure 15.7. Empirical models of **A.** density and **B.** modulus from compression graphed vs. total Si concentration and fraction of APTES-derived Si, and **C.** recovered strain graphed vs. total Si concentration and BTMSH fraction. Reprinted from [11], Copyright 2009 American Chemical Society.

It is possible to achieve good, i.e., nearly complete, recovery after compression with epoxy-reinforced aerogels using 15 mol% APTES, 40 mol% Si from *BTMSH*, and 15% (w/w) epoxy in the soaking solution; this is illustrated in Figure 15.7C. In fact, across the whole range of total Si concentration (densities ranging from 0.1 to 0.23 g/cm^3 and modulus as high as 10 MPa), the monoliths prepared using these conditions recover nearly their full length after deformation to 25% strain. Similar modulus and recovery after compression is obtained in epoxy reinforced aerogels using ethyl-linked or octyl-linked bis-silanes in place of BTMSH [36].

If more flexible monoliths are desired, vastly improved elastic recovery from compression at up to as much as 50% strain can be obtained using even lower total Si concentration (0.4 mol/l total Si, 45 mol% derived from APTES, and 40 mol% from BTMSH). As shown in Figure 15.8, a 2.3 cm monolith made using this formulation after

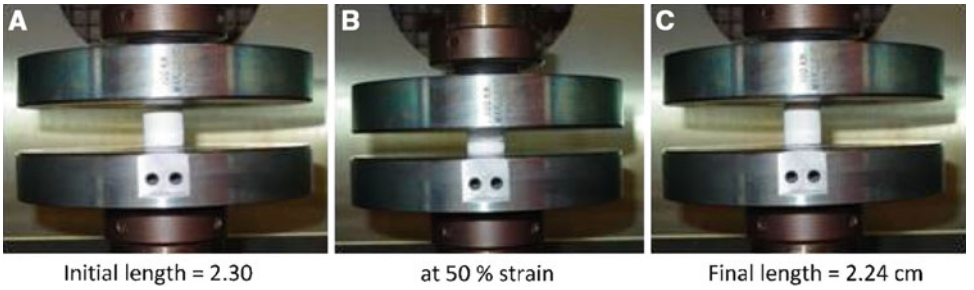

Figure 15.8. Repeat compression test to 50% strain of epoxy-reinforced monolith made using 0.4 mol/l total Si (40 mol% from BTMSH and 45 mol% from APTES). Reprinted from [11], Copyright 2009 American Chemical Society.

two compression cycles to 50% strain loses only 2.6% of initial length. At 25% strain, the sample demonstrates complete recovery after two compression cycles. However, with a density of 0.047 g/cm^3 and porosity greater than 96%, the modulus of this monolith decreases to 0.05 MPa and surface area is also low (54 m^2/g).

15.3. Alkyl Trialkoxysilane-Based Reinforced Aerogels

As pointed out in Sect. 15.1 of this chapter, *MTMS*-based aerogels have been synthesized with a surprising amount of flexibility [28, 29]. It is of interest then to see if strength and durability of the *MTMS* aerogels can be improved by introducing the notion of polymer reinforcement. In preliminary studies, formulations with *MTMS* coreacted with APTES to provide a reactive site for polymer cross-linking tend to gel in only a narrow range of total Si concentration and they shrink much more than their *TEOS*- or *TMOS*-based counterparts [37]. In contrast, *MTMS* coreacted with bis(trimethoxysilyl-propyl) amine (*BTMSPA*) readily gels across a wide range of total Si concentration [38]. The secondary amine of *BTMSPA* provides a ready reactive site for Desmodur N3300A [34], a tri-isocyanate cross-linker, as shown in Scheme 15.6.

Since only a small excess of water (ratio of water to Si ranging from 2 to 5) was used to make the aerogels in this study, chain extension of the polyurea was minimized. NMR analysis indicated that the polymer-reinforced structure is as shown with approximately a one-to-three ratio between each amine and each tri-isocyanate for samples where total Si ranged from 1.2 to 1.65 mol/l and 40 to 80 mol% of the Si from *BTMSPA*. For gels made in acetonitrile with lower total Si and 40 mol% *BTMSPA*, it was found that very little isocyanate cross-linking occurred. Monoliths made using these formulations also exhibited very low BET surface areas ($<$10 m^2/g), most likely due to solvent interactions between acetonitrile and polar surface groups. With methyl groups in greater abundance on the surface of the developing gel, this leads to collapse of the gel structure. Such low surface area would lead to very little secondary amine available to react with isocyanate. Using a less polar solvent such as acetone for gelation reverses this trend, leading to higher surface areas and better cross-linking.

Figure 15.9 shows a side-by-side comparison of unreinforced monoliths (left) and polymer-reinforced monoliths (right) produced using the same initial gelation conditions. All four monoliths pictured were prepared using 1.65 mol/l total Si. Figure 15.9A, B is of aerogel monoliths produced using 80 mol% Si derived from BTMSPA. As illustrated,

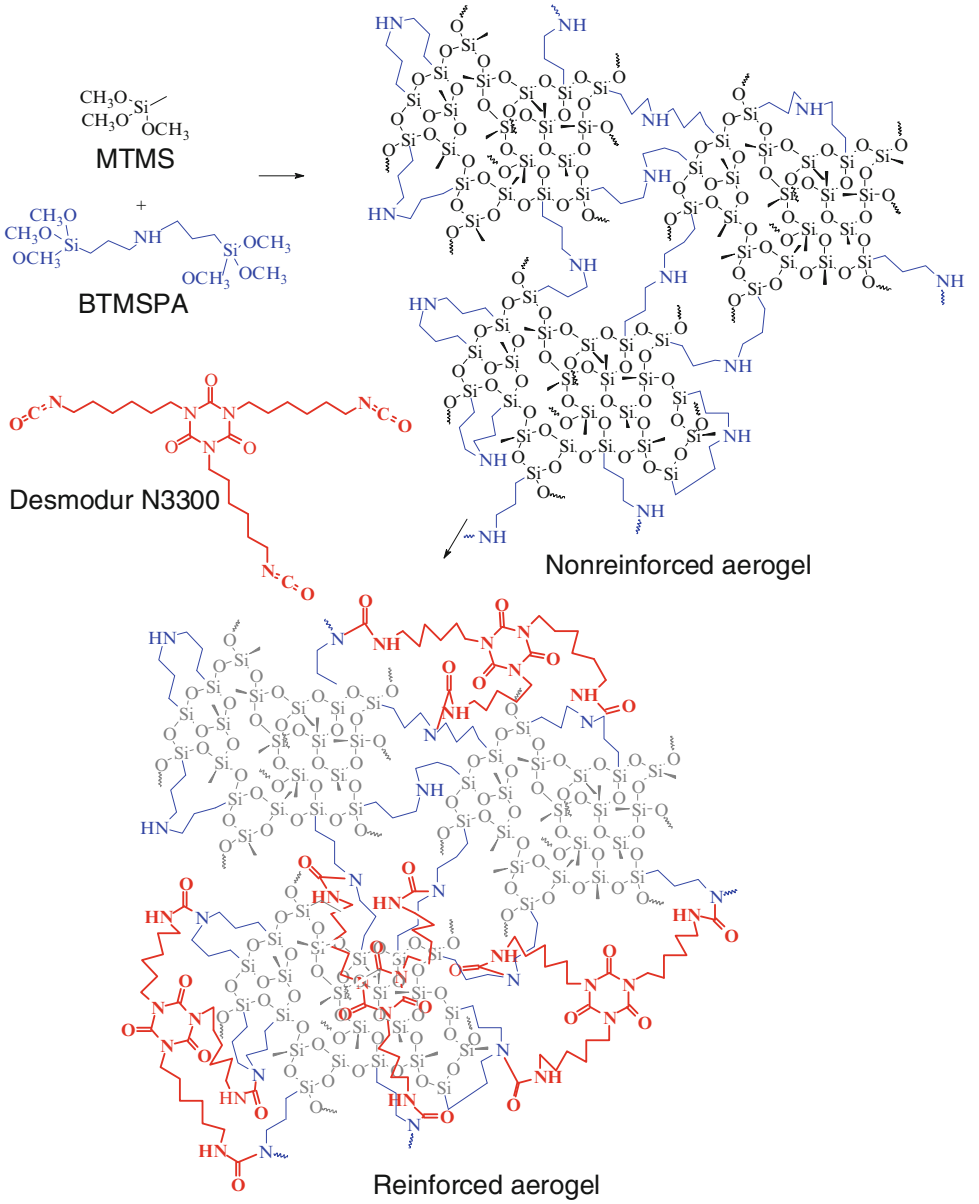

Scheme 15.6. Synthesis of MTMS-based aerogels with BTMSPA used as both a flexible linking group and site for tri-isocyanate crosslinking. Reprinted from [38], Copyright 2010 American Chemical Society.

particle sizes are very similar in appearance; however, the pores appear slightly reduced in size in the reinforced structure (Figure 15.9B). This accounts in part for the relatively large differences in density, porosity, and surface areas between the two samples. When BTMSPA mole fraction is reduced to 40 mol% (Figure 15.9C, D), both uncross-linked and polymer-reinforced aerogels exhibit a larger distribution of pore sizes than seen in Figure 15.9A, B, probably due to the different spacing formed from the connecting group in BTMSPA vs. the

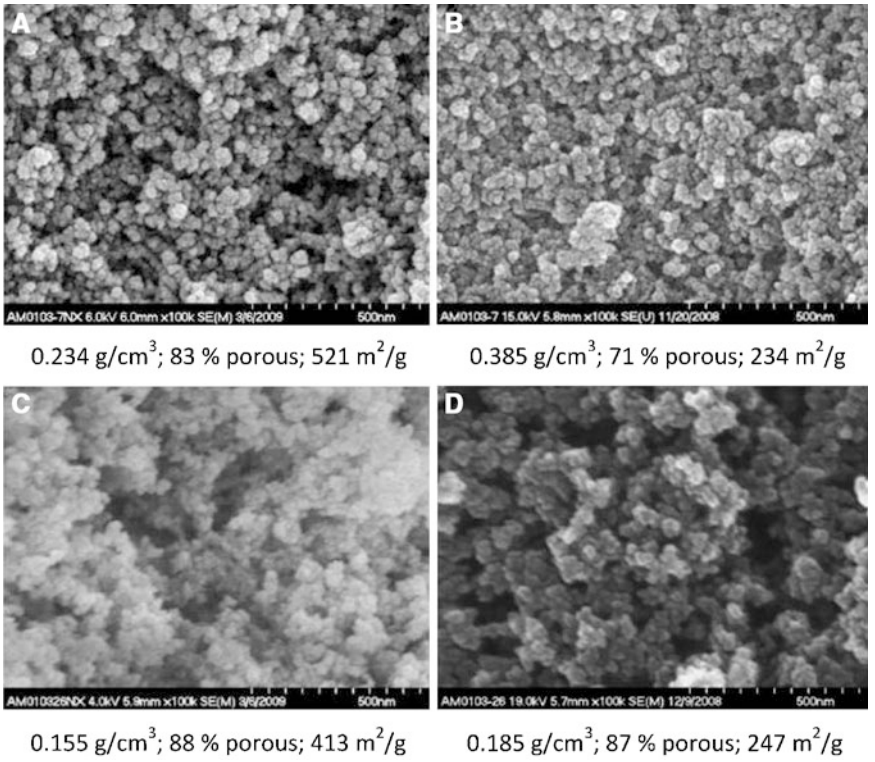

Figure 15.9. SEM images of aerogel monoliths made using 1.65 mol/l total Si: **A.** uncross-linked and **B.** polymer-reinforced aerogels prepared using 80 mol% Si from BTMSPA; and **C.** uncrosslinked and **D.** polymer-reinforced aerogels prepared using 40 mol% Si from BTMSPA. Reprinted from [38], Copyright 2010 American Chemical Society.

nonreactive methyl groups contributed by *MTMS*. Notably, the uncross-linked monolith in Figure 15.9C has a much finer particle structure and larger surface area than compared to the reinforced aerogel shown in Figure 15.9D (smoother, larger particles).

Compression testing of the monoliths made from MTMS and BTMSPA was carried out as previously described on both the unreinforced and polymer-reinforced aerogels. Though there is usually a trade-off between modulus and elastic recovery as seen with the hexyl-linked aerogels, in this study, the trade-off is very small, with even the highest modulus (84 MPa) of cross-linked aerogels exhibiting only about 3% unrecovered strain. To illustrate, stress–strain curves for repeat compression tests to 25% strain of four different polymer-reinforced aerogels are compared in Figure 15.10 (both graphs show the same four monoliths at different scales). The pairs of lines represent two subsequent stress–strain curves for each of the monoliths. The green curve labeled Test 1 is the first compression and Test 2 is the second compression for a formulation from 1.65 mol/l total Si (80 mol% from BTMSPA), with about 3% strain not recovered. In contrast, the red lines show repeated compression cycles from a formulation, made using 1.2 mol/l total Si but 80 mol% BTMSPA-derived Si. In this case, unrecovered strain is $<2\%$ (the sample recovers almost completely). Hence, a high degree of elastic recovery is present using a combination of MTMS-derived Si and the organic linking groups from BTMSPA.

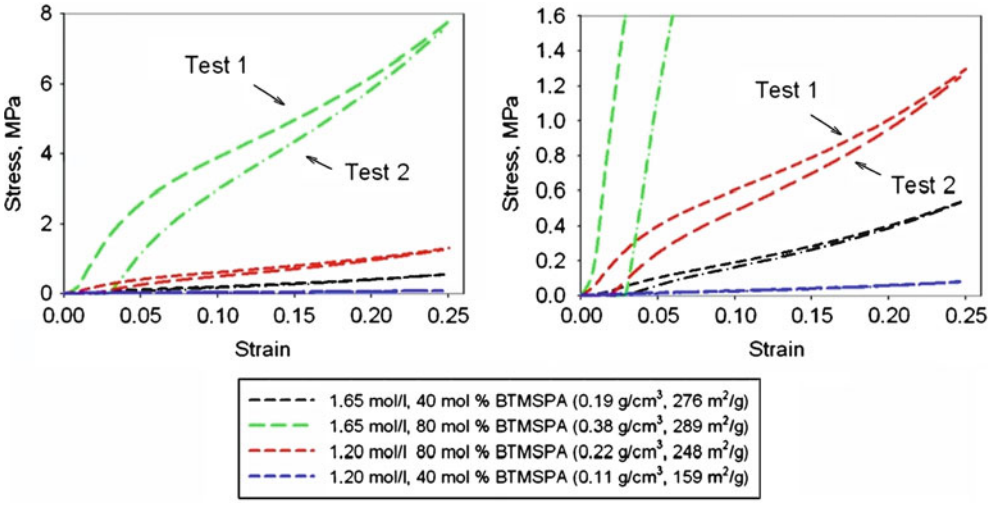

Figure 15.10. Typical stress–strain curves for a repeat compression tests on MTMS aerogels reinforced with Desmodur N3300A tri-isocyanate at different total silicon concentration and mol fraction of BTMSPA. The graphs are the same curves shown at different *y*-scales. Densities and surface areas of the monoliths made in acetonitrile are shown in *parentheses*. Reprinted from [38], Copyright 2010 American Chemical Society.

Unreinforced aerogels from the same study have about the same degree of recovery as the cross-linked aerogels shown.

Typical compressive stress–strain curves taken to failure are shown in Figure 15.11A. For unreinforced aerogels, the Young's modulus taken from the initial slope of the stress–strain curve is typically about half of that for the reinforced aerogels. In addition, the unreinforced aerogels break at about half the value of strain and the maximum stress at break is an order of magnitude lower. Hence, as seen in the graph of the response surface model shown in Figure 15.11B, the toughness, calculated from the area under the stress strain

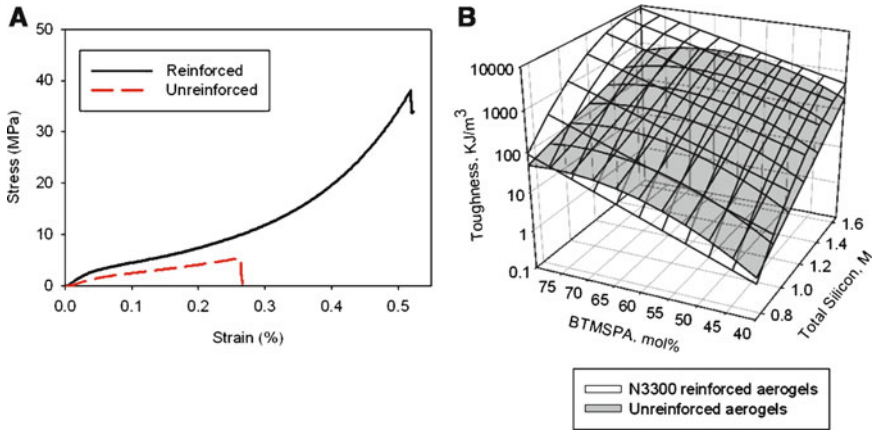

Figure 15.11. **A**. Typical stress–strain curve for compression to break and **B**. the response surface model of toughness calculated from the stress–strain curves for both crosslinked and uncrosslinked aerogel monoliths. Reprinted from [38], Copyright 2010 American Chemical Society.

curve, is as much as an order of magnitude higher for polyurea-reinforced aerogels made from *MTMS* and BTMSPA. Thus, while elastic recovery is about the same for reinforced and unreinforced aerogels using *MTMS* and BTMSPA, the polymer-reinforced aerogels are much more robust.

15.4. Future Directions

Incorporating flexible links in the silica backbone or using *MTMS* in place of *TEOS* in polymer-reinforced aerogels has been shown to be an effective way to introduce flexibility and good elastic recovery. In some cases, increasing the amount of polymer cross-linking does reduce flexibility. Thus, it stands to reason that in these cases the use of a more flexible polymer in combination with alterations made to the silica structure should increase flexibility even more. Taking this notion one step further, use of a shape memory polymer as reinforcement may give rise to a shape memory aerogel [39]. A shape memory polymer, such as a polyurethane block copolymer, is capable of changing its shape in response to a set of external stimuli, for example, pH, electric current, magnetic induction, and heating. Usually, one or more polymer blocks respond to the external stimuli, while others contribute to the desired properties. The synthesis of flexible aerogels reinforced with shape memory polyurethane cross-linkers should give rise to a shape memory effect as shown in Figure 15.12, offering the advantage of storage of the aerogel in a deformed state for transport aboard a spacecraft where storage is at a premium. Alternatively, the shape memory aerogel could be inserted into a cavity needing insulation in its deformed shape and made to recover to fill the cavity.

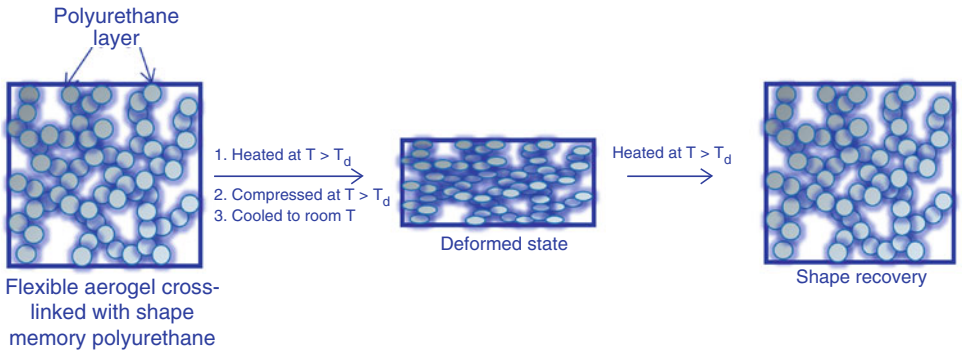

Figure 15.12. Proposed scheme to deploy a flexible aerogel reinforced with a shape memory polyurethane.

Flexible monolithic aerogels could have wide applications in various thermal insulation systems for space as previously discussed. For structures that need to be folded in a compact space for transport before deploying, such as the inflatable decelerators or habitats for the Moon or Mars, the thinner and more flexible the insulation system, the better. In such a thin form, even the polymer-reinforced aerogels with flexible linking groups as described in this chapter would probably be too fragile to stand on their own. Use of a continuous nonwoven fiber batting to further reinforce the flexible aerogels, such as in the aerogel blankets produced by Aspen Aerogels is one approach, but may still not result in a thin enough insulation for such deployable structures.

Carbon nanofiber-reinforced silica aerogel composites can be made by incorporating up to 5% (w/w) of the nanofibers into the initial sol [40]. Tensile strength of the composite aerogels using di-isocyanate as a polymer cross-link was improved by as much as a factor of 5 over di-isocyanate-cross-linked aerogels with no carbon nanofibers. In addition, the nanofiber containing gels were also easier to handle before cross-linking. Incorporating carbon nanofibers into a flexible reinforced aerogel matrix may allow the formation of thinner, more flexible aerogel sheets with improved durability (Chap. 36).

Another way to form a thin aerogel composite is to incorporate electrospun polyurethane nanofibers into a cast sol film prior to gelation of the silica-based sol [41]. By precisely controlling the gelation kinetics with the amount of base present in the formulation, nanofibers are electrospun into the sol before the onset of the gelation process and uniformly embedded in a silica network made flexible by incorporating low molecular weight oligomers of silanol-terminated *PDMS*. The final composite films, which have been fabricated to be 0.5–2 mm in thickness, are pliable and flexible as seen in Figure 15.13A. After much bending and pulling on the films by hand, small cracks develop, but as shown in Figure 15.13B, the film holds together by the nanofibers knitted together and bridging the crack. The room temperature thermal conductivity of the composite aerogels range from 13 mW/m-K for samples with bulk density of 0.17 g/cm^3 to 50 mW/m-K for samples with bulk density of 0.08 g/cm^3. Future work will involve optimization of the aerogel matrix and nanofiber chemistry, as well as nanofiber thickness to better reinforce the aerogel structure.

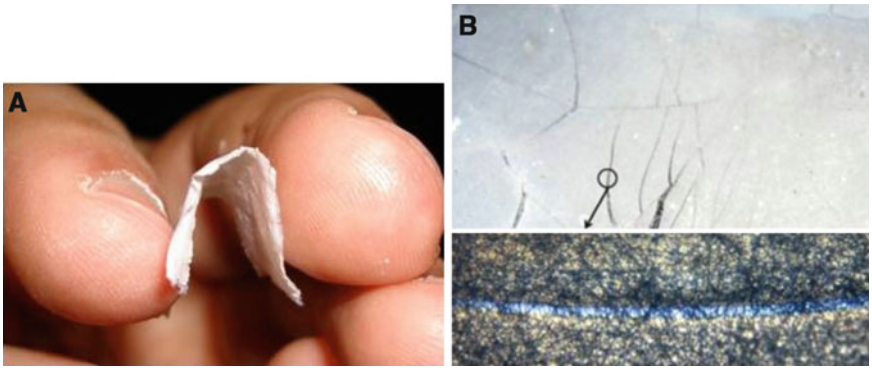

Figure 15.13. A. A 0.46 mm thick aerogel–nanofiber hybrid film bent almost 180°; **B.** microscope image of 2 mm thick aerogel sheet after excessive repetitive bending and pulling apart by hand. Reprinted from [41], Copyright 2009 American Chemical Society.

15.5. Conclusions

Incorporating short, flexible, organic linking groups into the silica backbone of polymer-reinforced aerogels has been shown to be a versatile way to improve elastic properties of the aerogels. The aerogels can recover from compression up to as much as 50% strain and in some cases are even flexible. The flexible linking groups may also result in greater hydrophobicity especially when combined with hydrophobic polymer cross-linkers such as polystyrene (Chap. 3) and also provide a means to tailor pore structure.

While there is a trade-off between modulus and elastic recovery in polymer-reinforced aerogels using flexible linking groups, the combination of *MTMS* and BTMSPA used in the

silica backbone provides enhanced elastic properties almost independent of modulus. These aerogels recover nearly all of their length after compression to 25% strain across the whole modulus range. Reinforcing these aerogels with tri-isocyanate oligomers reacted through the secondary amine of BTMSPA results in up to an order of magnitude increase in compressive strength and toughness of the aerogel monoliths, while the overall elastic properties arising from the underlying silica structure is maintained. Use of flexible polymer-cross-linked aerogels, especially in combination with nanofiber reinforcement is a promising route to making robust aerogel thin films and sheets, enabling a multitude of aerospace applications.

References

1. Pierre A C, Pajonk G M (2002) Chemistry of aerogels and their applications. Chem Rev 102: 4243–4265.
2. Fricke J (1998) Aerogels – Highly tenuous solids with fascinating properties. J Non-Cryst Solids 100: 169–173.
3. Husing N, Schubert U (1998) Aerogels – Airy materials: Chemistry, Structure and Properties. Angew Chem Int Ed 37: 22–45.
4. Parmenter K E, Milstein F (1998) Mechanical properties of silica aerogels. J. Non-Cryst Solids 223: 179–189.
5. Tsou P, Brownlee D E, Sandford S A, Hörz F, Zolensky M E (2003) Wild 2 and interstellar sample collection and Earth return. J Geophys Res 108(E10): 8113.
6. Jones S M (2006) Aerogel: Space exploration applications. J Sol-Gel Sci Tech 40: 351–357.
7. Zhang G, Dass A, Rawashdeh A-M M, Thomas J, Counsil J A, Sotiriou-Leventis C, Fabrizio E F, Ilhan F, Vassilaras P, Scheiman D A, McCorkle L, Palczer A, Johnston J C, Meador M A B, Leventis N (2004) Isocyanate-crosslinked silica aerogel monoliths: preparation and characterization. J. Non-Cryst Solids 350:152–164.
8. Leventis N, Sotiriou-Leventis C, Zhang G, Rawashdeh A-M M (2002) Nanoengineering Strong Silica Aerogels. Nano Lett 2: 957–960.
9. Boday D J, Stover R J, Muriithi B, Keller M W, Wertz J T, Obrey K A D, Loy D A (2008) Formation of Polycyanoacrylate–Silica Nanocomposites by Chemical Vapor Deposition of Cyanoacrylates on Aerogels. Chem Mater 20: 2845–2847.
10. Meador M A B, Fabrizzio E F, Ilhan F, Dass A, Zhang G, Vassilaras P, Johnston J C, Leventis N (2005) Cross-linking amine modified silica aerogels with epoxies: Mechanically strong lightweight porous materials. Chem Mater 17: 1085–1098.
11. Meador M A B, Weber A S, Hindi A, Naumenko M, McCorkle L, Quade D, Vivod S L, Gould G L, White S, Deshpande K (2009) Structure property relationships in porous 3D nanostructures: Epoxy cross-linked silica aerogels produced using ethanol as the solvent. ACS Appl Mater Interfaces 1: 894–906.
12. Boday D J, Stover R J, Muriithi B, Keller M W, Wertz J T, Obrey K A D, Loy D A (2009) Strong, Low-Density Nanocomposites by Chemical Vapor Deposition and Polymerization of Cyanoacrylates on Aminated Silica Aerogels. ACS Appl Mater Interfaces 1: 1364–1369.
13. Meador M A B, Capadona L A, Papadopoulos D S, Leventis N (2007) Structure property relationships in porous 3D nanostructures as a function of preparation conditions: Isocyanate cross-linked silica aerogels. Chem Mater 19: 2247–2260.
14. Capadona L A, Meador M A B, Alumni A, Fabrizzio E F, Vassilaras P, Leventis N (2006) Flexible, low-density polymer crosslinked silica aerogels. Polymer 47: 5754–5761.
15. Katti A, Shimpi N, Roy S, Lu H, Fabrizio E F, Dass A, Capadona L A, Leventis N (2006) Chemical, physical and mechanical characterization of isocyanate cross-linked amine modified silica aerogels. Chem Mater 18: 285–296.
16. Ilhan U F, Fabrizio E F, McCorkle L, Scheiman D A, Dass A, Palczer A, Meador M A B, Johnston J C, Leventis N (2006) Hydrophobic monolithic aerogels by nanocasting polystyrene on amine-modified silica. J Mater Chem 16: 3046–3054.
17. Mulik S, Sotiriou-Leventis C, Churu G, Lu H, Leventis N (2008) Cross-linking 3D assemblies of nanoparticles into mechanically strong aerogels by surface-initiated free-radical polymerization. Chem Mater 20: 5035–5046.
18. Nguyen B N, Meador M A B, Tousley M E, Shonkwiler B, McCorkle L, Scheiman D A, Palczer A (2009) Tailoring elastic properties of silica aerogels cross-linked with polystyrene. ACS Appl Mater Interfaces 1: 621–630.

19. Fidalgo A, Farinha J P S, Martinho J M G, Rosa M E, Ilharco L M (2007) Hybrid silica/polymer aerogels dried at ambient pressure. Chem Mater 19: 2603–2609.
20. Novak B M, Auerbach D, Verrier C (1994) Low-density mutually interpenetrating organic–inorganic composite materials via supercritical drying techniques. Chem Mater 6: 282–286.
21. Wei T Y, Lu S Y, Chang Y C (2008) Transparent, hydrophobic composite aerogels with high mechanical strength and low high-temperature thermal conductivities. J Phys Chem B 112: 11881–11886.
22. Essex Corporation, Extravehicular Activity in Mars Surface Exploration, Final Report on Advanced Extravehicular Activity Systems Requirements Definition Study (1989) NAS9–17779.
23. Paul H L, Diller K R (2003) Comparison Thermal Insulation Performance of Fibrous Materials for the Advanced Space Suit. J Biomechanical Engineering 125: 639–647.
24. Tang H H, Orndoff E S, Trevino L A (2006) Thermal performance of space suit elements with aerogel insulation for Moon and Mars exploration. 36th International Conference on Environment Systems, July 17–20, 2006, Norfolk, Virginia AIAA 2006–01–2235.
25. Fesmire J E (2006) Aerogel insulation systems for space launch applications. Cryogenics 46: 111–117.
26. Braun R D, Manning R M (2007) Mars Exploration Entry, Descent and Landing Challenges. J Spacecraft and Rockets 44: 310–323.
27. Brown G J, Lingard J S, Darley G D, Underwood J C (2007) Inflatable aerocapture decelerators for Mars Orbiters. 19th AIAA Aerodynamic Decelerator Systems Technology Conference and Seminar 21–24 May 2007, Williamsburg, VA, AIAA 2007–2543.
28. Reza S, Hund R, Kustas F, Willcockson W, Songer J (2007) Aerocapture Inflatable decelerator (AID) for planetary entry. 19th AIAA Aerodynamic Decelerator Systems Technology Conference and Seminar 21–24 May 2007, Williamsburg, VA, AIAA 2007–2516.
29. Kramer S J, Rubio-Alonso F, Mackenzie J D (1996) Organically Modified Silicate Aerogel: Aeromosil. Mat Res Soc Symp Proc 435: 295–299.
30. Rao A V, Bhagat S D, Hirashima H, Pajonk G M (2006) Synthesis of flexible silica aerogels using methyltrimethoxysilane (MTMS) precursor. J Colloid and Interface Sci 300: 279–285.
31. Kanamori K, Aizawa M, Nakanishi K, Hanada T (2006) New transparent methylsilsesquioxane aerogels and xerogels with improved mechanical properties. Adv Mater 19: 1589–1593.
32. Shea K J, Loy D A (2001) Bridged polysilsesquioxanes. Molecular-engineered hybrid organic–inorganic materials. Chem Mater 13: 3306–3319.
33. Loy D A, Shea K J (1995) Bridged Polysilsesquioxanes. Highly porous hybrid organic–inorganic materials. Chem Rev 95: 1431–1442.
34. Supplied by Bayer Corporation.
35. Vivod S L, Meador M A B, Nguyen B N, Perry R (2009) Flexible di-isocyanate cross-linked silica aerogels with 1,6-bis(trimethoxysilyl)hexane incorporated in the underlying silica backbone. Polym Preprints 50: 119–120.
36. Randall J P, Meador M A B, Jana S C (2011) Tailoring mechanical properties of aerogels for aerospace. ACS Appl Mater and Interfaces, 3: dx.doi.org/10.1021/am200007n.
37. Meador M A B, Nguyen B N, Scherzer C S unpublished results.
38. Nguyen B N, Meador M A B, Medoro A, Arendt V, Randall J, McCorkle L, Shonkwiler B (2010) Elastic behavior of methyltrimethoxysilane based aerogels reinforced with tri-isocyanate. ACS Applied Materials and Interfaces 2: 1430–1443.
39. Jana S C, Meador M A B, Randall J P (2008) Process for forming shape-memory polymer aerogel composites. US Patent Application, 2006–854838P.
40. Meador M A B, Vivod S L, McCorkle L, Quade D, Sullivan R M, Ghosn L J, Clark N, Capadona L A (2008) Reinforcing polymer cross-linked aerogels with carbon nanofibers. J Mater Chem 18: 1843–1852.
41. Li L, Yalcin B, Nguyen B N, Meador M A B, Cakmak M (2009) Nanofiber reinforced aerogel (xerogel): synthesis, manufacture and characterization. ACS Appl Mater and Interfaces, 1: 2491–2501.